Research article JHEP|Reports

Microbiota modulation by dietary oat beta-glucan prevents steatotic liver disease progression

Authors

Julius W. Jaeger, Annette Brandt, Wenfang Gui, Timur Yergaliyev, Angélica Hernández-Arriaga, Mukil Marutha Muthu, Karolina Edlund, Ahmed Elashy, Antonio Molinaro, Diana Möckel, Jan Sarges, Emina Halibasic, Michael Trauner, Florian Kahles, Ulrike Rolle-Kampczyk, Jan Hengstler, Carolin Victoria Schneider, Twan Lammers, Hanns-Ulrich Marschall, Martin von Bergen, Amélia Camarinha-Silva, Ina Bergheim, Christian Trautwein, Kai Markus Schneider

Correspondence

kmschneider@ukaachen.de (K.M. Schneider).

Graphical abstract

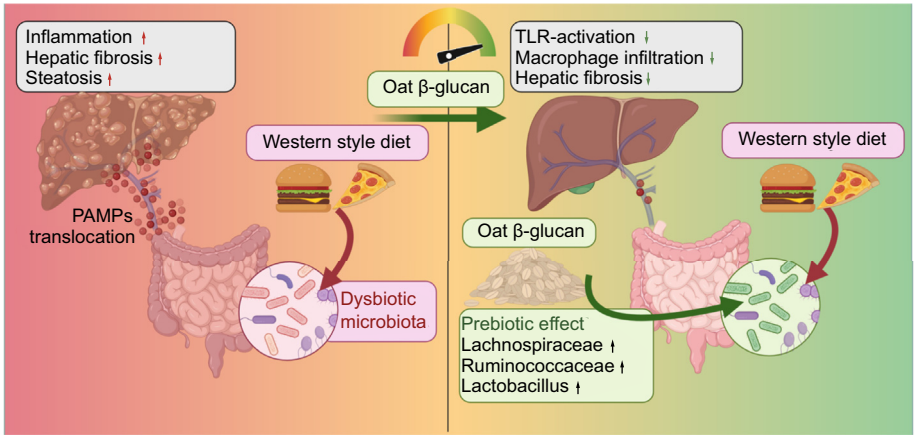

Highlights

- Oat beta-glucan exhibits a strong hepatoprotective effect in MASLD, especially against fibrosis progression.
- Supplementation of oat beta-glucan dampens infiltration of monocyte-derived macrophages and the PRR-driven innate immune response.
- Oat beta-glucan reshapes intestinal microbiota composition by promoting protective bacterial taxa to reduce translocation of TLR4 ligands.
- Bile acid composition remains largely unaffected by beta-glucan supplementation.

Impact and Implications

Herein, we investigated the effect of oat beta-glucan on the gut-liver axis and fibrosis development in a mouse model of metabolic dysfunction-associated steatotic liver disease (MASLD). Beta-glucan significantly reduced inflammation and fibrosis in the liver, which was associated with favorable shifts in gut microbiota that protected against bacterial translocation and activation of fibroinflammatory pathways. Together, oat beta-glucan may be a cost-effective and well-tolerated approach to prevent MASLD progression and should be assessed in clinical studies.

https://doi.org/10.1016/j.jhepr.2023.100987

Research article

JHEP|Reports

Microbiota modulation by dietary oat beta-glucan prevents steatotic liver disease progression

Julius W. Jaeger,[1] Annette Brandt,[2] Wenfang Gui,[1] Timur Yergaliyev,[3] Angélica Hernández-Arriaga,[3] Mukil Marutha Muthu,[3] Karolina Edlund,[4] Ahmed Elashy,[1] Antonio Molinaro,[5,6] Diana Möckel,[7] Jan Sarges,[1] Emina Halibasic,[8] Michael Trauner,[8] Florian Kahles,[9] Ulrike Rolle-Kampczyk,[10] Jan Hengstler,[4] Carolin Victoria Schneider,[1] Twan Lammers,[6] Hanns-Ulrich Marschall,[5,†] Martin von Bergen,[10] Amélia Camarinha-Silva,[3] Ina Bergheim,[2] Christian Trautwein,[1,‡] Kai Markus Schneider[1,*,‡]

[1]*Department of Medicine III, University Hospital RWTH Aachen, Aachen, Germany;* [2]*Department of Nutritional Sciences, University of Vienna, Vienna, Austria;* [3]*Department Microbial Ecology of Livestock at the Institute of Animal Science, University of Hohenheim, Stuttgart, Germany;* [4]*Department of Toxicology, Leibniz Research Centre for Working Environment and Human Factors, Dortmund, Germany;* [5]*Wallenberg Laboratory, Department of Molecular and Clinical Medicine and Sahlgrenska Center for Cardiovascular and Metabolic Research, University of Gothenburg, Gothenburg, Sweden;* [6]*Norwegian PSC Research Center, Department of Transplantation Medicine, Oslo University Hospital Rikshospitalet, Oslo, Norway;* [7]*Institute for Experimental Molecular Imaging (ExMI), RWTH Aachen University, Aachen, Germany;* [8]*Division of Gastroenterology and Hepatology, Department of Internal Medicine III, Medical University of Vienna, Vienna, Austria;* [9]*Department of Medicine I, University Hospital RWTH Aachen, Aachen, Germany;* [10]*Department of Molecular Systems Biology, Helmholtz Centre for Environmental Research (UFZ), Leipzig, Germany*

JHEP Reports **2024.** https://doi.org/10.1016/j.jhepr.2023.100987

Background & Aims: Changes in gut microbiota in metabolic dysfunction-associated steatotic liver disease (MASLD) are important drivers of disease progression towards fibrosis. Therefore, reversing microbial alterations could ameliorate MASLD progression. Oat beta-glucan, a non-digestible polysaccharide, has shown promising therapeutic effects on hyperlipidemia associated with MASLD, but its impact on gut microbiota and most importantly MASLD-related fibrosis remains unknown.
Methods: We performed detailed metabolic phenotyping, including assessments of body composition, glucose tolerance, and lipid metabolism, as well as comprehensive characterization of the gut-liver axis in a western-style diet (WSD)-induced model of MASLD and assessed the effect of a beta-glucan intervention on early and advanced liver disease. Gut microbiota were modulated using broad-spectrum antibiotic treatment.
Results: Oat beta-glucan supplementation did not affect WSD-induced body weight gain or glucose intolerance and the metabolic phenotype remained largely unaffected. Interestingly, oat beta-glucan dampened MASLD-related inflammation, which was associated with significantly reduced monocyte-derived macrophage infiltration and fibroinflammatory gene expression, as well as strongly reduced fibrosis development. Mechanistically, this protective effect was not mediated by changes in bile acid composition or signaling, but was dependent on gut microbiota and was lost upon broad-spectrum antibiotic treatment. Specifically, oat beta-glucan partially reversed unfavorable changes in gut microbiota, resulting in an expansion of protective taxa, including *Ruminococcus*, and *Lactobacillus* followed by reduced translocation of Toll-like receptor ligands.
Conclusions: Our findings identify oat beta-glucan as a highly efficacious food supplement that dampens inflammation and fibrosis development in diet-induced MASLD. These results, along with its favorable dietary profile, suggest that it may be a cost-effective and well-tolerated approach to preventing MASLD progression and should be assessed in clinical studies.
Impact and Implications: Herein, we investigated the effect of oat beta-glucan on the gut-liver axis and fibrosis development in a mouse model of metabolic dysfunction-associated steatotic liver disease (MASLD). Beta-glucan significantly reduced inflammation and fibrosis in the liver, which was associated with favorable shifts in gut microbiota that protected against bacterial translocation and activation of fibroinflammatory pathways. Together, oat beta-glucan may be a cost-effective and well-tolerated approach to prevent MASLD progression and should be assessed in clinical studies.

Keywords: MASLD; beta-glucan; microbiota; fibrosis; gut-liver axis; prebiotics.
Received 7 May 2023; received in revised form 16 November 2023; accepted 6 December 2023; available online 3 January 2024
† Deceased.
‡ Equal contribution
* Corresponding author. Address: Department of Medicine III, University Hospital, RWTH Aachen, Pauwelsstraße, 30, Aachen 52074, Germany. Tel.: +49-241-80-8037727, fax: +49-241-80-37727.
E-mail address: kmschneider@ukaachen.de (K.M. Schneider).

Introduction

Metabolic dysfunction-associated steatotic liver disease (MASLD) has become the most prevalent liver disease globally and its prevalence is steadily increasing.[1] The absence of efficient FDA-approved medication makes clinical management of MASLD difficult despite recent improvements in our knowledge of the underlying disease mechanisms.[2] At present, although long-term

adherence is poor, lifestyle modification is successful in patients who are compliant.

Emerging evidence suggests that gut microbiota play a key role in the development and progression of liver disease.[3] The microbiome has a vast enzymatic repertoire facilitating a wide range of metabolic processes in the gut and liver, such as bile acid metabolism[4] and the production of short-chain fatty acids (SCFAs). Gut microbiota also control intestinal barrier function and dysbiosis has been associated with gut barrier dysfunction in patients with MASLD. Increased translocation of bacterial components such as lipopolysaccharides from the gut into the liver may trigger an innate immune response that drives disease progression towards fibrosis.[5] In patients with MASLD, beneficial modification of the gut microbiota may have the potential to slow progression of fibrosis and inflammation.

Beta-glucans are a group of non-digestible polysaccharides found in fungi, yeast, and cereals. Depending on their source, beta-glucans can have different characteristics in terms of solubility, viscosity, and physiological effects in the host.[6] Oat beta-glucan can be fermented by the intestinal microbiome, which produces SCFAs and affects gut microbiome composition, acting as a prebiotic.[7] Beta-glucan also has significant effects on bile acid metabolism and composition. By hindering the intestinal reabsorption of bile acids and increasing bile acid synthesis, beta-glucan has been shown to alter bile acid composition and signaling within the gut-liver axis.[8,9] Previous studies have explored the therapeutic potential of beta-glucan in other components of the metabolic syndrome, its cholesterol-lowering properties and its effect on hepatic steatosis.[10]

To date, there have been no studies on the effect of oat beta-glucan on late-stage MASLD, specifically its effect on hepatic fibrosis development. Therefore, the present study aimed to investigate the potential protective effects of oat beta-glucan on the development of MASLD beyond metabolic changes and intrahepatic lipid accumulation. Additionally, this study examined the influence of beta-glucan on the intestinal microbiome, bile acid composition, and its role as a prebiotic.

Materials and methods

Mouse model

All experiments were approved by the appropriate German authorities (LANUV, NorthRhine-Westphalia, AZ-84-02.04.2017.A327) and conducted according to the criteria outlined in the "Guide for the Care and Use of Laboratory Animals" published by the National Institutes of Health (publication 86-23, revised 1985). Only male C57BL/6J were used. All animals were housed under specific pathogen-free conditions and a 12 h/12 h light/dark cycle at a constant temperature of 20-24 °C. Hepatic steatosis was induced by feeding the mice with a western standard diet (WSD) or chow diet for 8 or 24 weeks, respectively. The WSD was obtained from Brogaarden Research (D16022301, rodent diet with 40 kcal% fat [mostly non-trans-fat Primex], 20 kcal % fructose and 2% cholesterol). All animal experiments were performed twice. The collection of tissue and blood samples, and serum parameters were determined as described previously.[11]

Oral beta-glucan treatment

Beta-glucan (Soluble Oat Fiber [70% oat-beta-glucan] Gluten Free, Garuda, Exeter, USA) was administered via drinking water at a concentration of 1 g of beta-glucan per kg bodyweight assuming a daily water intake of 4 ml.

Broad-spectrum antibiotic treatment

Mice were treated with four broad-spectrum antibiotics (1 g/L ampicillin [Ratiopharm, Ulm, Germany], 160 mg/L gentamicin [Panpharma GmbH, Trittau, Germany], 1 g/L metronidazole [B. Braun, Melsungen, Germany], 1 g/L vancomycin [Dr. Eberth, Urensohn, Germany]).

Intraperitoneal glucose tolerance test

One week prior to sacrifice, mice were fasted for 6 h and then intraperitoneally injected with 2 mg glucose (Glucose 40% B.Braun, Melsungen, Germany) per g bodyweight. Blood sugar was measured after 15 min, 30 min, 1 h and 2 h from tail blood using a blood glucose meter (ACCU-Check Advantage Glucose monitoring Test system, Roche Diabetes Care GmBH, Mannheim, Germany).

In vivo microcomputed tomography imaging

High-resolution microcomputed tomography (μCT) (U-CT, MILabs B.V., Utrecht, The Netherlands) was performed to acquire a total body μCT scan with two subscans to cover the entire animal. In a full-rotation in step-and-shoot mode, 480 projections (1,944 × 1,536 pixels) were acquired with an X-ray tube voltage of 55 kV, power 0.17 mA, exposure time of 75 ms, and low-dose (≈0.1 Gy/whole body scan). All acquired 3D μCT images were reconstructed at an isotropic voxel size of 80 μm using a Feldkamp type algorithm (filtered backprojection). For fat-containing tissue, 3D organ segmentations were generated based on the μCT data using interactive segmentation operations (Imalytics Preclinical, Gremse-IT GmbH, Aachen, Germany;[12]).

Triglyceride assay

Analysis of intrahepatic triglyceride concentration was performed via the Triglycerides Liquicolor kit (Human, Wiesbaden, Germany), according to the manufacturer's protocol.

H&E staining

H&E staining was performed according to a standard protocol.[5] Samples were deparaffinized and rehydrated. Next, the sections were treated with Mayer's hematoxylin (Sigma, Steinheim, Germany) for 1 minute. Samples were then rinsed in water for 15 minutes, set in distilled water for 30 s and 95% alcohol for 30 s. Next, they were counterstained with eosin (Sigma, Steinheim, Germany) solution. Finally, cuts were dehydrated and mounted with coverslips using Roti® Histokit (Carl Roth, Karlsruhe, Germany).[13]

Oil Red O staining

Cryo-conserved liver tissue sections were cut to 7 μm thickness. Sections were fixed in paraformaldehyde. Next, sections were incubated in Oil Red O dying solution (36% Oil Red O [Sigma, Steinheim, Germany] in 60% isopropanol) for 1 hour and washed. For counterstaining of cell nuclei, sections were treated with Mayers hematoxylin (Sigma, Steinheim, Germany).

Immunohistochemistry staining

Liver tissue was fixed in paraffin and cut to 5 μm thickness. Initially the cuts were deparaffinized, rehydrated and heated in citrate buffer (pH 6.0). Sections were treated with H_2O_2 solution (3% in water). Specimens were blocked for 20 min with a 1:1 solution of fetal bovine serum, PBS and 3% bovine serum albumin and incubated overnight with the primary antibody (CD 45, BD biosciences, Franklin Lakes, US). On the following day, slides

were washed with PBS and subsequently treated with a secondary antibody for 2 h with the ImmPRESS Polymer Kit (Vector Labratories, San Francisco, USA). Finally, target signals were visualized using 3,3′-diaminobenzidine solution (Vector Laboratories, Burlingame, CA, USA) for 2–5 min under the microscope.

Sirius red staining

Tissue sections were deparaffinized and rehydrated. Next, tissue sections were placed in 0.1% Sirius red (Direct Red 80, Sigma Aldrich, Munich, Germany) solution (2 g Sirius Red F 3B in 200 ml picric acid) for 45 min, followed by incubation in 0.5% glacial acetic acid for 2 × 15 s. Finally, sections were dehydrated and mounted with coverslips using Roti® Histokit. Collagen deposition was quantified by area fraction analysis (ImageJ; National Institutes of Health, Bethesda, MD).

Flow cytometry analysis of intrahepatic leukocytes

Flow cytometry was performed according to standard protocol.[5] The same amounts of liver tissue were digested by collagenase type IV (Roche Diagnostics GmbH, Mannheim, Germany) for 2 h and intrahepatic leukocytes were isolated through multiple differential centrifugation steps as previously published.[14] Samples were blocked with blocking buffer for 30 min. Immune cell extracts were stained with fluorochrome-conjugated antibodies of either a myeloid panel against CD11b (BV421; eBioscience, Frankfurt, Germany; 12-0112-82), CD45 (APC-Cy7; BD Biosciences, Erlangen, Germany; 557659), F4/80 (PE-Cy7; eBioscience, Frankfurt, Germany; 25-4801-82), Ly6G (AlexaFlour 700; Biolegend, San Diego, USA; 127622) or lymphoid panel against CD3 (APC; eBioscience, Frankfurt, Germany; 17-0031-82), CD4 (BV421; eBioscience, Frankfurt, Germany; 48-0041-82), CD8 (FITC; eBioscience, Frankfurt, Germany; 11-0081-85), CD19 (Alexa Flour 700; BD Biosciences, Erlangen, Germany; 551001), CD45 (APC-Cy7; BD Biosciences, Erlangen, Germany; 557659). Absolute cell numbers were determined by adding fixed numbers of Calibrite APC beads (BD Biosciences, Erlangen, Germany) as internal reference. Analysis was performed using FACS LSR Fortessa (BD Biosciences, Erlangen, Germany) and the acquired data was analyzed with FlowJo software (TreeStar, Ashland, OR).

Quantitative real-time PCR

RNA was isolated from liver tissue specimens using Trizol reagent (Life Technologies, Carlsbad, CA) according to the manufacturer's protocol. RNA concentrations were measured by NanoDrop ND-1000 UV-Vis (Thermo Scientific, Waltham, USA) and reverse transcription was conducted using an Omniscript RT kit (Qiagen, Hilden, Germany) according to the manufacturer's protocol. Fast SYBR GreenER Master Mix (Thermo Fisher, Waltham, USA) was used to conduct real-time PCR reactions according to the manufacturer's recommendations using Real-Time PCR System 7300 (Applied Biosystems, Darmstadt, Germany). The following primer sequences were used for GAPDH (5'-AGGGCTGCTTTTAACTCTGGT-3', 3'-CCCCACTTGATTTTGGAGGGA-5'), CCl2 (5'-AGCTGTAGTTTTTGTCACCAAGC-3', 3'-TTCCTTCTT GGGGTCAGCAC-5'), CCl5 (5'-GCTGCTTTGCCTACCTCTCC-3', 3'-TCGAGTGACAAACACGACTGC-5'), Col1 (5'-GCTACTACCGGGCC-GATGATGC-3', 3'-CCTTCGGGGCTGCGGATGTTC-5'), aSMA (5'-TCCTCCCTGGAGAAGAGCTAC-3', 3'-TATAGGTGGTTTCGTGGATGC-5'), TLR4 (5'-TTCAGAACTTCAGTGGCTGGATT-3', 3'-CCATGC CTTGTCTTCAA TTGTTT-5'), TLR9 (5'-AATCCCTCATATCCCTGTCCC-3', 3'-GTTGCCGTCCATGAATAGGAAG-5'). QuantStudio Flex software (ThermoFisher Scientific, Waltham, USA) was used for analysis. Expression of mRNA of the target gene was calculated using the 2−ΔΔCT method, relative to the expression of GAPDH.

Immunoblotting

Protein was isolated from liver tissue according to standard protocol in NP40-Lysis buffer.[11] Concentrations were measured via Bradford assay (Bio-Rad, Hercules, USA) and normalized to 2 μg/μl. Then Laemmli buffer was added and protein samples were denatured at 96 °C for 10 min. The protein samples were separated via electrophoresis on precast 4%-12% polyacrylamide gel (Bio-Rad, Hercules, USA) while submerged in sodium dodecyl sulfate running buffer at 140 mV. Next, separated proteins were transferred to a nitrocellulose membrane via Trans-Blot Turbo Transfer System (Trans-Blot Turbo Transfer Pack 0.2 μm Nitrocellulose, Bio-Rad, Hercules, USA). A successful transfer of protein was confirmed by staining with Ponceau Red (Sigma, Steinheim, Germany). Then samples were incubated with 5% non-fat dry milk dissolved in tris-buffered saline tween (TBST) to block non-specific binding sites and treated with the primary antibody (Col1A1, 91144, Cell signaling, Danvers, USA; GAPDH, MCA4739, Bio-Rad, Hercules, USA) diluted in TBST overnight at 4 °C. On the next day, the membrane was washed with TBST and incubated with the horseradish peroxidase-conjugated secondary antibody (anti-rabbit for 1 h at room temperature). Next, the membrane was washed and incubated in ECL substrate (Pierce, Waltham, USA). The membrane was developed using LAS mini 4000 (Fuji, Tokyo, Japan).[11]

HEK-Blue™ mTLR4 cells

Toll-like receptor 4 (TLR4) ligands were measured using the HEK-Blue™ mTLR4 Cell assay (Invivogen, San Diego, USA) according to the manufacturer's protocol. Next, cells were challenged with serum samples and TLR4 activity was determined by measuring the secreted embryonic alkaline phosphatase-induced color change of cell culture medium at 655 nm.[15]

DNA isolation and 16S rRNA gene amplicon sequencing

Fecal DNA isolations and 16S rRNA sequencing were performed as previously described[16] using the Trizol protocol (Trizol, Sigma Aldrich, Darmstadt, Germany). Sequencing libraries were prepared by targeting the V4 region of the 16S rRNA gene. Master mix was prepared by using PrimeSTAR® HS DNA Polymerase kit (TaKaRa, Beijing, China) with a total volume of 25 μl for first and second PCR and 50 μl for the third PCR, containing 2 μl of DNA template, 0.2 μM Primer and 0.5 U Taq primer star HS DNA (TaKaRa, China). The PCR conditions consisted of an initial denaturation at 95 °C for 3 min, followed by 10 cycles for the first and second PCR and 20 cycles for the third PCR according to protocol: 98 °C denaturation for 10 s, annealing at 55 °C for 10 s and extension at 72 °C for 45 s followed by a final extension at 72 °C for 2 min. Following normalization via the SequalPrep Normalization Kit (Invitrogen Inc., Carlsbad, CA, USA), libraries were sequenced on an Illumina MiSeq platform. Bioinformatical part of the metabarcoding analysis was performed with Qiime2.[17] Demultiplexing was performed by Sabre (GitHub - najoshi/sabre, 2023-04-29)[18] and primers were removed by q2-cutadapt.[19] Raw reads denoising and merging were carried out by the q2-dada2.[20] Taxonomy was assigned using RESCRIPt[21] and VSEARCH-based consensus[22] and pre-fitted sklearn-based[23] classifiers *vs.* SILVA (v.138.1, 16S 99%)[24] database. All organelle

DNA sequences were removed. A phylogenetic tree was created by the q2-phylogeny plugin, implementing MAFFT 7.3 for sequence alignment,[25] and FastTree 2.1[26]. Beta diversity was assessed by Bray-Curtis distances,[27] which were subsequently used for principal coordinate analysis.[28] Beta diversity differences between groups of samples were tested with the adonis test.[29] The LEfSe[30] algorithm was used to identify differentially abundant features.

RNA isolation and RNA sequencing

RNA was isolated using the PureLink RNA Mini Kit (Invitrogen, Carlsbad, CA, USA). RNA concentrations were measured on a Qubit 4 Fluorometer with the RNA BR Assay Kit (Thermo Fisher, Waltham, USA) and RNA integrity was assessed on a 2100 Bioanalyzer with the RNA 6000 Nano Kit (Agilent Technologies). Sequencing libraries were generated from 500 ng of RNA, using the TruSeq Stranded mRNA Kit with unique dual indexes (Illumina, San Diego, CA, USA), according to the manufacturer's protocol. Quantification of the final libraries was performed with the Qubit 1X dsDNA HS Assay Kit (Thermo Fisher, Waltham, USA), and library sizes were checked on an Agilent 2100 Bioanalyzer with the DNA 1000 Kit (Agilent Technologies, Santa Clara, CA, USA). The libraries were then normalized, pooled, diluted to 1.0 pM, and paired-end sequenced (2x75 bp) using the 500/550 High Output Kit v2.5 (Illumina, San Diego, CA, USA) on an Illumina NextSeq 550.

Pseudo-alignment was performed using Salmon v1.10.1,[31] allowing for the efficient quantification of transcript-level abundances. The resulting data was organized and metadata was managed using Tximeta v1.16.1,[32] for downstream analysis. The DESeq2 v1.38.3[33] negative binomial distribution model was utilized to perform differential gene expression analysis, identifying genes with differential expression across sample groups. Prior to principal component analysis, the raw count data was normalized using the vst() function in DESeq2. Functional enrichment analysis was carried out with clusterProfiler v4.6.0,[34] incorporating genome-wide annotation from org.Mm.eg.db[35] v3.16.0, and the enrichment results were visualized using the enrichplot package v1.18.3.[36] Additionally, heatmaps were generated for data visualization with the gplots package v3.1.3,[37] and data manipulation and visualization were performed using the tidyverse package v2.0.0.[38] All analyses were conducted in R version 4.2.2.

Statistical analysis

All data are expressed as mean ± standard deviation. Data analysis was conducted with GraphPad Prism (San Diego, USA) software version 9. Significance was tested using one-way ANOVA followed by Sidak's-test with adjusted p values for multiple comparisons. In case of non-normally distributed data, significance was tested via Kruskal-Wallis test with Dunn's test. Data were considered significant between groups at p <0.05.

Results

Beta-glucan prevents liver weight gain without affecting body composition

To investigate the potential protective effect of beta-glucan on MASLD progression, we treated C57BL/6 mice with a WSD, a well-established mouse model that leads to an increase in body weight and pathological fat tissue distribution.[39–41] Mice received either normal drinking water or drinking water supplemented with oat beta-glucan at a concentration of 1 g of beta-glucan per kg bodyweight. After 24 weeks, all mice fed a WSD had significantly increased body weight compared to controls, while the beta-glucan intervention did not affect weight gain (Fig. 1A,B). As previously shown, WSD treatment elevated the liver-to-body-weight-ratio, indicating increased liver remodeling and fibrogenesis.[42] Importantly, this effect was partially reversed in mice receiving beta-glucan, suggesting a protective effect against hepatic remodeling (Fig. 1C).

To evaluate the distribution of fat tissue, we performed CT scans 1 week prior to sacrifice. As expected, the mice showed increased overall body fat, subcutaneous and visceral fat after WSD. However, none of these fat compartments were significantly affected by beta-glucan supplementation (Figs 1D-G and Fig. S1).

Beta-glucan does not affect lipid metabolism and glucose tolerance

To test whether beta-glucan supplementation may affect lipid metabolism, we first measured serum total cholesterol levels. As expected, WSD treatment significantly increased cholesterol levels, but they were not lowered by beta-glucan treatment (Fig. 2A). To study intrahepatic lipid accumulation, we performed Oil Red O staining and quantified the abundance of hepatic triglycerides in liver tissue with a colorimetric triglyceride assay. WSD was associated with markedly increased macro- and microsteatosis revealed upon Oil Red O staining, without any differences regarding fat vacuole configuration in the groups treated with beta-glucan (Fig. 2B). Moreover, triglyceride concentrations in hepatic tissue were significantly increased after WSD, with no change after the beta-glucan intervention (Fig. 2C,D).

We further performed an intraperitoneal glucose tolerance test to examine the potential influence of beta-glucan on glucose tolerance as another clinical feature of the metabolic syndrome. As previously shown,[43] WSD feeding induced glucose intolerance, reflected by a significant increase in the area under the curve in the glucose tolerance test (Fig. 2E-G). Importantly, there was no noticeable effect of the beta-glucan intervention in the control and WSD groups. Additionally, we analyzed critical metabolic pathways in the liver to assess the potential influence of beta-glucan on molecular metabolic signaling. In line with our previous findings, WSD led to a significant increase in the mRNA expression of *Ppara*, *Cd36* and *Srebp*, *Chrebp*. However, we could not detect a significant effect of beta-glucan treatment on these pathways (Fig. S2A-E).

Collectively, these data indicate that the metabolic phenotype, including body fat distribution, hepatic fat accumulation, serum lipids as well as glucose tolerance remained largely unaffected by the beta-glucan intervention; and that the observed differences in the liver-to-body-weight ratio are potentially not due to changes in hepatic fibrotic remodeling upon beta-glucan supplementation.

Beta-glucan intervention ameliorates liver injury in MASLD

In order to investigate the potential protective effect of beta-glucan on the development of MASLD, we next assessed serum markers for liver injury at two independent time points (8 and 24 weeks). After only 8 weeks of treatment, serum levels of liver enzymes alanine aminotransferase (ALT), aspartate aminotransferase (AST), glutamate dehydrogenase (GDLH) and alkaline phosphatase were unchanged in all groups (Fig. S3A-D).

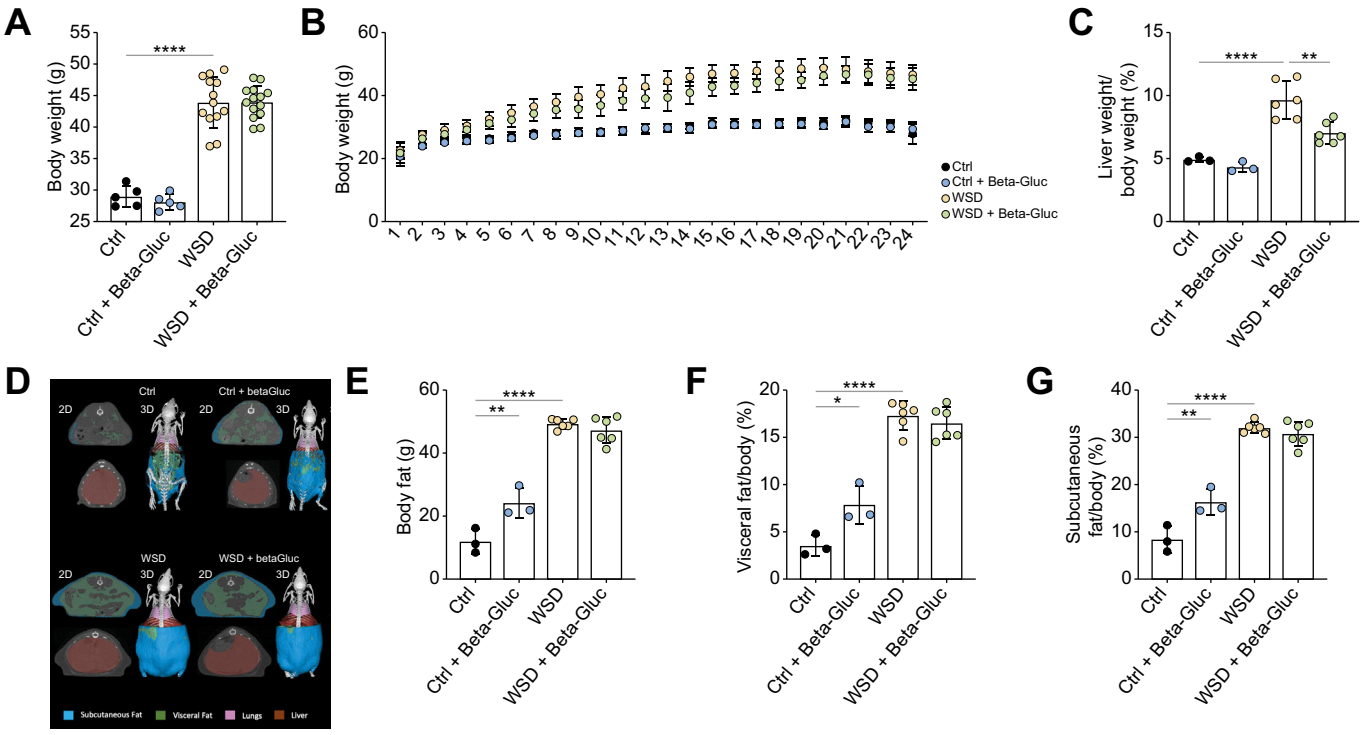

Fig. 1. Metabolic phenotype remains unaffected by treatment with beta-glucan. (A) Total body weight at termination. (B) Weight development throughout the 24-week long experiment. (C) Liver-body weight ratio at termination. (D) Representative cross-sectional images of μCT-scans. (E–G) μCT-analysis of total body fat, subcutaneous and visceral fat compartments. Data expressed as mean ± SD. Each dot represents one mouse. All statistical significance was assessed by one-way ANOVA followed by Sidak's multiple comparisons test. Experiments are considered significant at $^{*}p$ <0.05, $^{**}p$ <0.01 $^{***}p$ <0.001, and $^{****}p$ <0.0001. μCT, microcomputed tomography; WSD, western standard diet.

As previously shown, WSD treatment resulted in significantly elevated levels of ALT, AST, and GLDH after 24 weeks. At this timepoint, the beta-glucan intervention protected from liver injury as evidenced by decreased AST, ALT, and GLDH levels (Fig. 3A,B and Fig. S3E).

Beta-glucan decreases hepatic leukocyte infiltration, especially of the MoMFs

In order to explore how beta-glucan supplementation improves liver injury in WSD-induced MASLD, we conducted a liver RNA sequencing analysis. Using principal component analysis, we compared the global gene expression signatures and observed that WSD led to a shift in the transcriptomic profile of all groups, along principal component 1 (Fig. 3C). Interestingly, the WSD + beta-glucan group exhibited a distinct clustering pattern, located between the WSD and control groups that were on a normal chow diet. Next, we specifically focused on the comparison between WSD *vs.* WSD + beta-glucan groups. Proinflammatory genes associated with leukocyte recruitment such as *Ccl2* and *Ccr2* were significantly downregulated after beta-glucan treatment (Fig. 3D).

To explore global changes in transcriptomic programs upon beta-glucan supplementation in an unbiased way, we performed gene set-enrichment analysis. Interestingly, this analysis uncovered a suppression of pathways involved in inflammation, leukocyte and specifically myeloid cell migration, chemotaxis, and fibrosis (Fig. 3E), possibly contributing to reduced myeloid cell infiltration after beta-glucan supplementation. To validate the results from RNA sequencing analysis, we characterized immune cell infiltration using H&E-stained liver sections as well as immunohistochemistry against the pan leukocyte marker CD45. Intrahepatic leukocyte infiltration was significantly increased after WSD. This phenotype was ameliorated upon beta-glucan intervention (Fig. 3F,G). Aiming to differentiate specific leukocyte subpopulations, we analyzed hepatic myeloid and lymphoid cell populations using flow cytometry (Fig. S4). Whereas lymphoid cell populations including B cells, T cells and natural killer cells remained largely unchanged (Fig. S5), myeloid cell populations showed significant changes (Fig. 3H-K). After WSD, mice showed increased neutrophils, monocyte-derived macrophages (MoMFs), and Kupffer cells (Fig. 3H-K). Importantly, MoMFs and Kupffer cells were significantly reduced after beta-glucan treatment (Fig. 3J-K). MoMFs have been identified as essential drivers of steatohepatitis that are recruited in a *Ccl2*- and *Ccl5*-dependent fashion.[44] Consistently, beta-glucan supplementation significantly reduced levels of *Ccl2* and *Ccl5* expression in WSD-fed animals (Figs 3D,L-M, and S6).

Beta-glucan reduces hepatic fibrosis progression

Liver fibrosis is a clinically meaningful endpoint of MASLD. We, therefore, characterized hepatic fibrosis development using various orthogonal approaches. First, the deposition of fibrotic fibers was visualized using Sirius red staining, which allowed for the quantification of intrahepatic collagen networks (Fig. 4A). Collagen deposition was markedly increased after WSD, while beta-glucan treatment strongly ameliorated collagen abundance

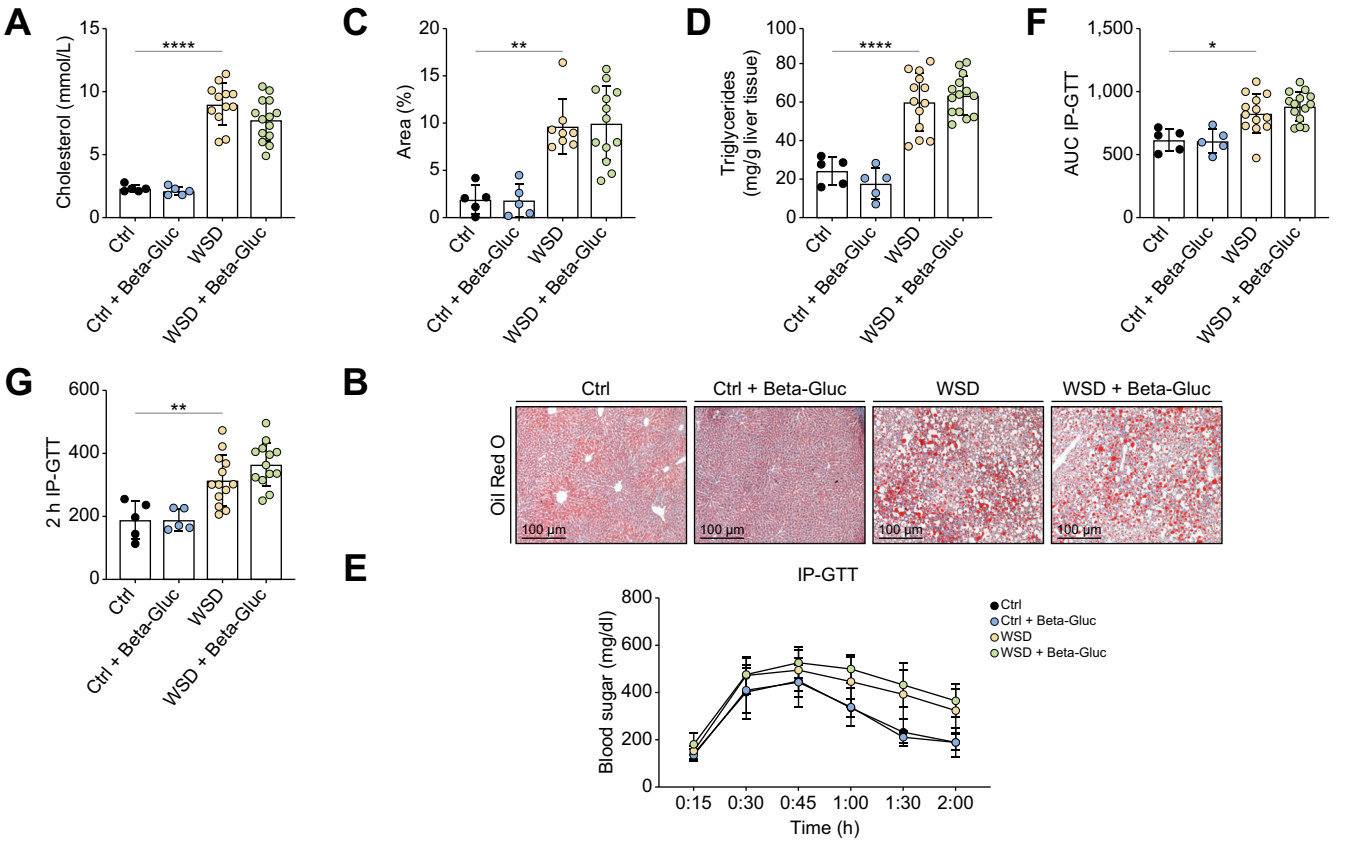

Fig. 2. Hypercholesterolemia, hepatic steatosis and glucose tolerance are independent of beta-glucan. (A) Serum cholesterol levels at termination. (B) Representative pictures of Oil Red O staining. (C) Area percentage of Oil Red O staining (Kruskal-Wallis test followed by Dunn's multiple comparisons test). (D) Triglyceride concentration in liver tissue. (E) Blood glucose levels after intraperitoneal glucose injection one week prior to sacrifice. (F) Area under the curve of IP-GTT. (G) Glucose levels two hours post injection. Each dot represents a singular one mouse. Data expressed as mean ± SD. All Statistical significance was assessed by one-way ANOVA followed by Sidak's multiple comparisons test. Experiments are considered significant at $^{*}p$ <0.05, $^{**}p$ <0.01 $^{***}p$ <0.001, and $^{****}p$ <0.0001. IP-GTT, intraperitoneal glucose tolerance test; µCT, microcomputed tomography; WSD, western standard diet.

(Fig. 4A,B). Next, protein expression of Col1 in hepatic tissue was assessed by western blotting. In line with Sirius red staining, protein expression of Col1 in hepatic tissue was significantly reduced in beta-glucan-treated mice (Fig. 4C,D). Consistently, *aSma* mRNA expression was significantly increased after WSD and strongly reduced in the beta-glucan-treated animals (Fig. 4E). Further, we performed a more comprehensive analysis of profibrotic genes through RNA sequencing. We observed that various genes involved in hepatic fibrosis development were downregulated in the mice that received beta-glucan (Fig. 4F).

Beta-glucan treatment does not affect bile acid composition

Previous reports have shown that beta-glucan may alter bile acid metabolism.[9] To investigate the potential influence of beta-glucan on the gut-liver axis via bile acids, we first measured distinct bile acid species in different compartments using high-performance liquid chromatography-tandem mass spectrometry. While mice fed with a WSD showed a significant increase of total bile acids in cecum stool, feces and systemic circulation, there was no notable difference after beta-glucan treatment (Fig. S7). There were no major differences between interventional groups. In addition, we analyzed *Fxr* expression in liver and intestinal tissue and *Cyp7a1* as a key enzyme in bile acid metabolism. In line with these data, there was no significant effect of beta-glucan treatment on bile acid metabolism (Fig. S8).

Beta-glucan alleviates intestinal dysbiosis after WSD

Since bile acid composition remained unchanged by beta-glucan treatment, we studied other molecular mechanisms mediating its hepatoprotective effects.

In previous studies beta-glucan has been identified as a potent prebiotic.[7] We hypothesized that the hepatoprotective effect of beta-glucan may result from its influence on gut microbiota. To investigate whether the intestinal microbiota might mediate this effect, we subsequently assessed intestinal microbiota composition using 16S rRNA gene amplicon sequencing.

Ordination analysis based on Bray-Curtis dissimilarity revealed distinct clustering of each group, suggesting profound effects of both diet and beta-glucan intervention on microbiome composition (Fig. 5A). To identify the responsible features driving the differences between the groups, we performed a linear discriminant analysis effect size analysis. This analysis revealed an increased abundance of features assigned to Lachnospiraceae, Ruminococcaceae and *Lactobacillus* in beta-glucan-treated animals compared to the WSD group (Fig. 5B). Notably

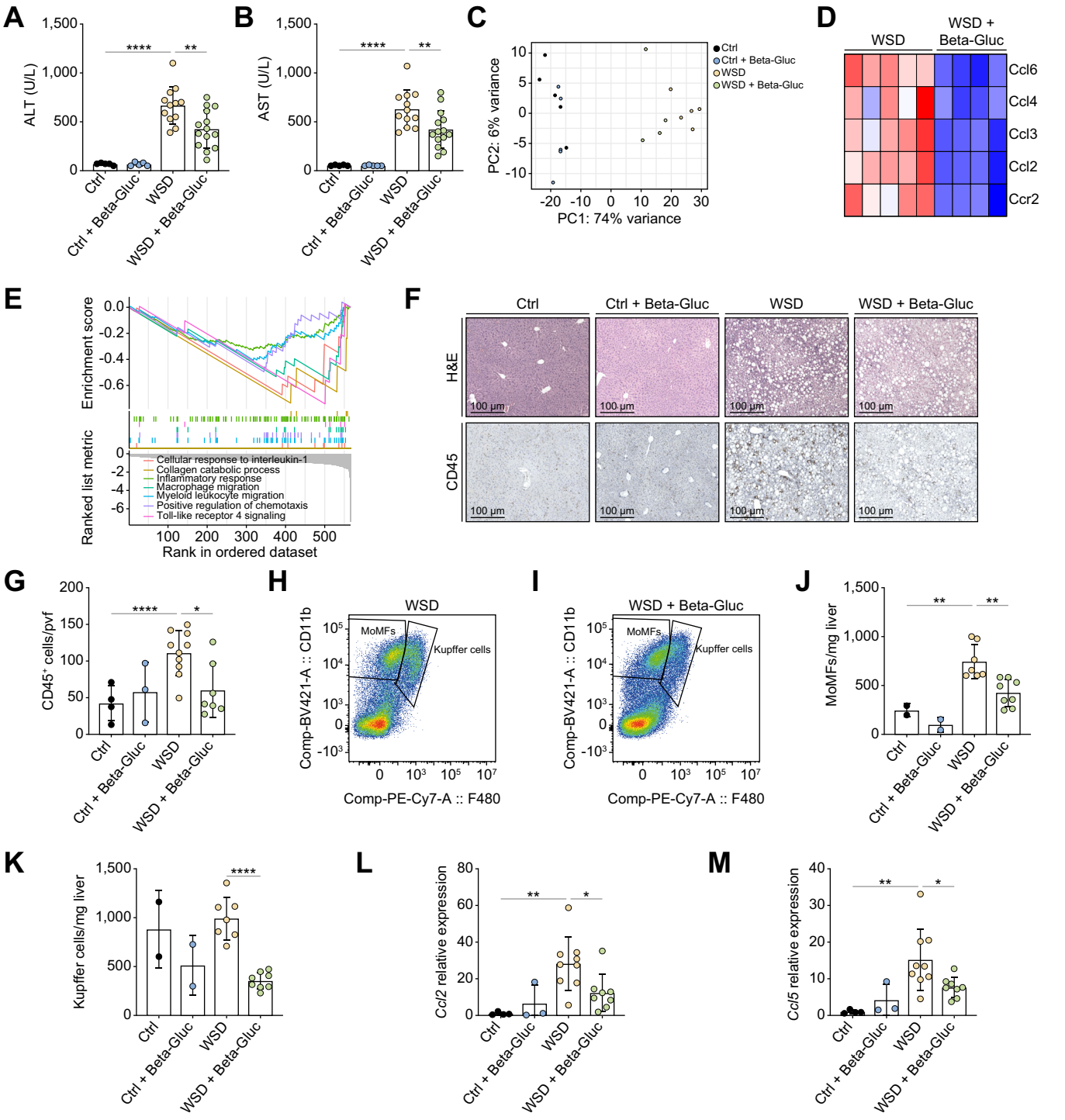

Fig. 3. Beta-glucan ameliorates liver damage and hepatic inflammation in MASLD. (A-B) Serum transaminases at termination. (C) PCA plot of transcriptomics. (D) Heatmap of differentially expressed proinflammatory genes from WSD *vs.* WSD + beta-glucan. (E) Gene set enrichment of differential expression of proinflammatory and collagen catabolic pathways from WSD mice *vs.* WSD + beta-glucan. (F-G) Representative pictures of H&E and CD45 stains. (H–K) FACS analysis of intrahepatic abundance of MoMFs and Kupffer cells. (L-M) *CCl2* and *CCl5* mRNA levels expressed as fold induction over control. Each dot represents one mouse. Data expressed as mean ± SD. All Statistical significance was assessed by one-way ANOVA followed by Sidak's multiple comparisons test. Experiments are considered significant at $^{*}p$ <0.05, $^{**}p$ <0.01 $^{***}p$ <0.001, and $^{****}p$ <0.0001. ALT, alanine aminotransferase; AST, aspartate aminotransferase; MASLD, metabolic dysfunction-associated steatotic liver disease; MoMFs, monocyte-derived macrophages; PCA, principal component analysis; WSD, western standard diet.

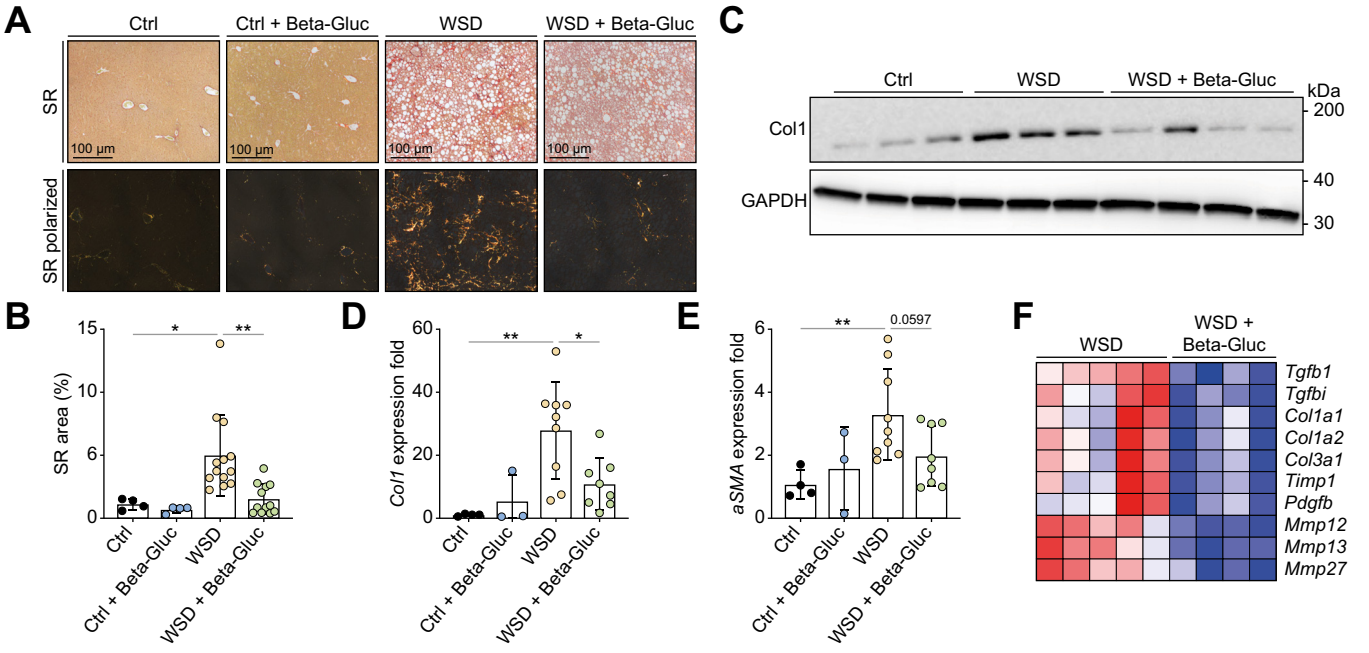

Fig. 4. Beta-glucan decreases hepatic fibrosis. (A) Representative images of SR staining. (B) Area stained by SR under polarization (Kruskal-Wallis test followed by Dunn's multiple comparisons test). (C-D) Protein and mRNA expression of Col1. (E) *aSMA* mRNA expressed as fold induction over control. (F) Heatmap of differentially expressed profibrotic genes from WSD *vs.* WSD + beta-glucan. Each dot represents a single mouse. Data expressed as mean ± SD. Statistical significance was assessed by one-way ANOVA followed by Sidak's multiple comparisons test unless stated otherwise. Experiments are considered significant at $^{*}p$ <0.05, $^{**}p$ <0.01 $^{***}p$ <0.001, and $^{****}p$ <0.0001. SR, Sirius red; WSD, western standard diet.

all of the afore mentioned features were more abundant in the control group compared to the WSD group (Fig. S9). Therefore, beta-glucan intervention seemed to partially restore gut microbiota integrity after WSD (Fig. 5C). Importantly, the identified taxa have been associated with an increased production of SCFAs.[45] To assess whether treatment with beta-glucan leads to a subsequent increase in SCFAs, we measured the levels of butyrate, propionate, and acetate in stool. The mice that had been treated with WSD showed significantly reduced total SCFAs, as well as reduced levels of acetate and propionate individually (Fig. S6). Consistent with its effect on the intestinal microbiota, beta-glucan led to increased levels of total SCFAs and individual levels of acetate, propionate, and butyrate. However, this effect reached significance for the total amount of SCFAs and butyrate only in the cohorts that had been fed a control diet (Fig. S10).

Intestinal dysbiosis is often linked to increased intestinal translocation of pathogen-associated molecular patterns (PAMPs) and metabolites through the venous drainage of the portal vein into the liver.[5,11] To determine whether the changes in intestinal microbiota composition induced by beta-glucan promoted bacterial translocation, we measured TLR4 ligands in serum via an mTLR4-cell-based assay. TLR4 ligands were significantly increased after WSD feeding. Importantly, the group receiving the beta-glucan intervention showed significantly lower amounts of TLR4 ligands compared to the WSD group (Fig. 5D).

Bacterial translocation results in the activation of pathogen recognition receptors, which have been shown to drive MASLD progression.[5] Therefore, we measured hepatic expression of *Tlr4* and *Tlr9*. Expression of both was markedly decreased after beta-glucan intervention. However, only *Tlr9* expression reached the level of significance (Fig. 5D-F). In line with these data, our transcriptomic data revealed that the pathway "response to external stimulus" was among the top downregulated pathways in the gene set-enrichment analysis. Notably, we found significant downregulation of proinflammatory genes, including genes involved in PAMP recognition, antigen presentation and innate immune response, in the beta-glucan cohort compared to the WSD cohort (Fig. 5G).

Together, the beta-glucan intervention partially reversed the WSD-induced unfavorable changes in microbiota composition, associated with reduced translocation of PAMPs and hepatic expression of pathogen recognition receptors, subsequently ameliorating hepatic inflammation.

Beta-glucan's hepatoprotective effect is microbiota dependent

To further dissect whether the intestinal microbiome is necessary for the observed hepatoprotective effects, we depleted gut microbiota with broad-spectrum antibiotics via drinking water. While both the antibiotic treatment and the double intervention of beta-glucan combined with oral antibiotics showed a significant reduction in liver injury markers and fibrosis, the double intervention failed to show an additional effect compared to the exclusive antibiotic intervention. Interestingly, beta-glucan treatment even resulted in significantly higher liver injury, evidenced by GLDH levels as well as a trend towards higher transaminases and fibrosis (Fig. 5H-J).

Together, these data suggest that the hepatoprotective effect of beta-glucan largely relies on the presence of intestinal microbiota and beta-glucan's ability to shape its composition in a prebiotic manner.

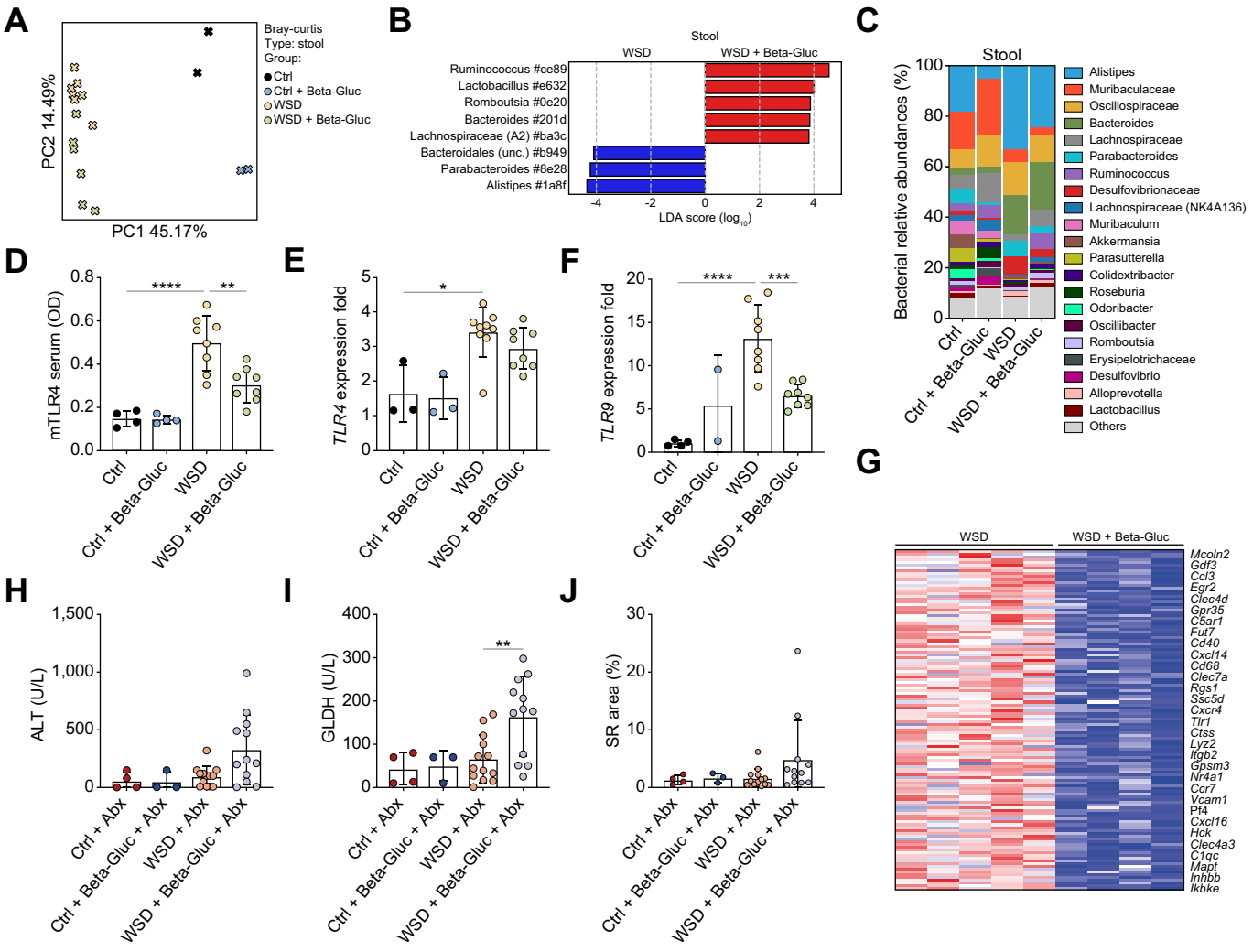

Fig. 5. Beta-glucan exhibits hepatoprotective prebiotic effects which are lost after microbiota depletion. (A) Ordination analysis based on Bray-Curtis distances of 16S rRNA sequencing of stool samples. (B) Linear discriminant analysis effect size analysis identifies differentially abundant features between WSD *vs.* WSD + beta-glucan group. (C) Relative abundance of bacterial taxa based on 16S rRNA sequencing. (D) TLR4 ligands in serum measured via HEK-Blue™ mTLR4 Cell assay. (E) *TLR4* mRNA expressed as fold induction over control (Kruskal-Wallis test followed by Dunn's multiple comparisons test). (F) *TLR9* mRNA expressed as fold induction over control. (G) Heatmap of the "response to external stimulus"-pathway from WSD *vs.* WSD + beta-glucan. (H-I) ALT and GLDH serum levels of mice treated with Abx (J) Area stained by SR under polarization (Kruskal-Wallis test followed by Dunn's multiple comparisons test). Each dot represents one mouse. Data expressed as mean ± SD. Statistical significance was assessed by one-way ANOVA followed by Sidak's multiple comparisons test unless stated otherwise. Experiments are considered significant at $^{*}p<0.05$, $^{**}p<0.01$ $^{***}p<0.001$, and $^{****}p<0.0001$. Abx, broad-spectrum antibiotics; GLDH, glutamate dehydrogenase; SR, Sirius red; WSD, western standard diet.

Discussion

MASLD is the most common liver disease worldwide and its prevalence continues to rise. Despite its epidemiological relevance, clinical management of MASLD still poses challenges due to the limited range of therapeutic agents.[2]

Previous studies have identified oat beta-glucan as a potent treatment option for other entities of the metabolic syndrome. In cases of hypercholesterolemia,[46] pathological glucose tolerance[47] and hepatic steatosis[48] it has proven to be a cost-effective and well-tolerated therapeutic alternative. Yet most studies to date have been conducted with fungi-derived beta-glucan and focused on earlier disease stages like intrahepatic steatosis.[49] Evidence regarding the potential hepatoprotective effect of oat beta-glucan, especially on later stages of MASLD, such as steatohepatitis or fibrosis, remains scarce. Thus, we treated mice for a duration of 24 weeks to gain an understanding of its role in late-stage MASLD.

Ho *et al.* who performed a meta-analysis of randomized-controlled trials investigating the effect of beta-glucan on serum cholesterol levels, observed a lowering effect of beta-glucan on LDL-cholesterol, non-HDL-cholesterol and apoB.[50] Interestingly we were unable to reproduce the previously published effects of beta-glucan on other entities of the metabolic syndrome. This might be explained by the longer duration of our experiment. While the majority of previously conducted studies had a maximum duration of 13 weeks,[51] our study aimed to assess advanced stages of MASLD and was therefore performed over nearly twice the length of time of previously published

studies. Hence, we propose that the beneficial effects of beta-glucan on the animal's metabolism might be overruled by chronic exposure to a WSD. Further, most other studies included beta-glucan as a part of the solid foods the mice consumed, while in our study we ensured the daily intake of beta-glucan via drinking water. As part of a solid diet, beta-glucan is associated with increased fiber intake, which might have caused early satiety in mice and consequently lower caloric intake. This hypothesis is supported by a previous study published by Vitaglione *et al.* who observed increased feelings of satiety and reduced food ingestion in probands following a diet with supplemented beta-glucan.[52] In addition, beta-glucan slows the gastric passage and reduces glycemic and insulinemic responses.[53] By performing an intraperitoneal glucose tolerance test instead of an oral administration of glucose we bypassed the gastric route and were able to exclude it as a confounder. As we were unable to reproduce previously published findings regarding the improvement of pathological glucose tolerance after beta-glucan treatment, we concluded this effect might be reliant on the gastric passage.

To study the molecular mechanisms underlying beta-glucan's effect on disease progression in MASLD, with a particular focus on the gut-liver axis, we analyzed the composition of the intestinal microbiota. Notably, we observed an increase in Lachnospiraceae, Ruminococcaceae, and *Lactobacillus* species following beta-glucan treatment. These bacteria are known to produce SCFAs.[54] We analyzed the concentration of SCFAs in stool to assess whether these changes in microbial composition also lead to increased levels of SCFAs. Notably, we found increased levels of total SCFAs and butyrate in mice that had received the beta-glucan intervention. SCFAs have been shown to modulate metabolic pathways and act as anti-inflammatory agents in MASLD.[55]

Previous studies have shown contrasting roles of single microbial agents in MASLD, specifically Ruminococcaceae. Boursier *et al.* observed a significantly increased abundance of the *Ruminococcus* genus in patients with higher degrees of hepatic fibrosis.[56] Contrasting to these findings Lee *et al.* reported that supplementation with Lachnospiraceae and Ruminococcaceae can protect against obesity, inflammation, intestinal dysbiosis, and hepatic fibrosis in MASLD,[57] which aligns with our findings of increased abundance of features assigned to these families following beta-glucan treatment and the resultant improvement in MASLD progression.[58] Other studies have further challenged the potential role Ruminococcaceae as a driver of MASLD.[59,60] These dichotomous findings are explained by the heterogenous spectrum of the *Ruminococcus* genus.[56] In our study we observed a significant reduction of *Ruminococcus* in the mice that had been fed WSD in comparison to the control group. This shift was partially reversed after beta-glucan treatment, which further indicates its role as a part of a homeostatic intestinal microbial composition.

Furthermore, we observed a reduced abundance of TLR4 ligands in the serum and reduced hepatic TLR expression in mice treated with beta-glucan, which suggests a decrease in bacterial translocation due to restored intestinal homeostasis. Previous studies have identified TLR4 ligands as an essential driver for intrahepatic fibrosis through the recruitment of Kupffer cells and hepatic stellate cells.[61] This is further supported as we observed a significant reduction in MoMFs and Kupffer cells, which are well-established drivers of MASLD progression.[44,62] Additionally, mice that had been treated with beta-glucan exhibited a significantly reduced expression of hepatic TLR9, a pattern recognition receptor that recognizes bacteria-derived cytosine phosphate guanine-containing DNA. TLR9 activation is linked to increased activation of the innate immune system, specifically Kupffer cells and reduced downstream production of IL-1β which further mediates intrahepatic fibrosis development.[63]

Thus, we concluded that beta-glucan restores intestinal microbial composition, reversing WSD-associated dysbiotic changes and exhibiting pleiotropic effects on the gut-liver-axis through microbial derived products like SCFAs and PAMPs. To further investigate whether gut microbiota are necessary for the observed therapeutic effect, we treated mice with oral broad-spectrum antibiotics. Interestingly, albeit the protective effect of each single treatment with beta-glucan or antibiotic, respectively, the combination of both treatments did not have a synergistic effect but instead resulted in slightly increased liver injury.

The data from our study suggest that beta-glucan could be a promising therapeutic agent for patients suffering from MASLD. Previous research on the efficacy of beta-glucan as a therapy for hypercholesterolemia has already demonstrated that it is well-tolerated and cost-effective in humans. Consequently, in 2010, the EFSA (European Food Safety Authority) Panel on Dietetic Products, Nutrition and Allergy issued a scientific opinion on the scientific substantiation of a health claim related to these important findings as follows, "Oat beta-glucan has been shown to lower/reduce blood cholesterol. Blood cholesterol lowering may reduce the risk of (coronary) heart disease". Further, they stipulate that in order to bear this claim, foods should provide at least 3 g of oat beta-glucans (EFSA Panel on Dietetic Products, Nutrition and Allergies, 2010).[64] A small human study also showed that an intake of 3 g of oat beta-glucans spread out in two portions per day is associated with a significant reduction of ALT and AST in the serum of overweight individuals with signs of altered liver function.[65] Our study extends these findings to advanced stages of liver disease and indicates a protective effect against fibrosis progression.

Our study was limited through employment of a single mouse model. In order to further elaborate on potential fibrosis-specific effects of beta-glucan, further experiments potentially in a specific model of liver fibrosis (*e.g.* carbon tetrachloride) would be beneficial. Wang *et al.* investigated the potential effect of beta-glucan on the development of hepatocellular carcinoma in a diethylnitrosamine/carbon tetrachloride model, however without the assessment of fibrosis development.[66] Targeted measurement of SCFAs revealed changes in their abundance after beta-glucan treatment in mice on chow diet, whereas SCFAs were only mildly elevated in mice on WSD. While translocation of PAMPs and subsequent signaling pathways were strongly dampened by beta-glucan, our data cannot exclude a contribution of other mechanisms (*e.g.*, via SCFAs or other metabolites) by which beta-glucan may reduce inflammation and fibrosis. Finally, to translate our findings to humans, well-controlled randomized-controlled trials are needed.

In summary, we describe a previously unknown hepatoprotective effect of oat beta-glucan on MASLD, specifically on fibrosis development, and provide a mechanistic explanation for its efficacy. Beta-glucan partially reversed intestinal dysbiosis and lowered circulating TLR-agonists with a subsequent decrease in innate immune responses in the liver. This effect was dependent on the intestinal microbiota.

Therefore, our study identifies oat beta-glucan as a potential novel therapeutic agent to prevent MASLD fibrosis by reshaping the gut microbiota.

Abbreviations

ALT, alanine aminotransferase; AST, aspartate aminotransferase; GLDH, glutamate dehydrogenase; MASLD, metabolic dysfunction-associated steatotic liver disease; MoMFs, monocyte-derived macrophages; PAMPs, pathogen-associated molecular pattern molecules; SCFAs, short-chain fatty acids; TLR, Toll-like receptor; μCT, microcomputed tomography; WSD, western standard diet.

Financial statement

This study was supported by the German Research Foundation CRC1382, A08 and B09 (Project-ID 403224013), DFG Tr 285/10-2 to C.T., the Federal Ministry of Education and Research (ObiHep grant #01KU1214A to C.T.), The HDHL-INTIMIC Di-Mi-Liv to C.T., I.B. A.S., K.M.S. and H.U.M., BMBF Knowledge Platform on Food, Diet, Intestinal Microbiomics and Human Health to C.T., the Interdisciplinary Centre for Clinical Research (START Grant #691438) within the Faculty of Medicine at RWTH Aachen University, the Swedish Research Council to H.U.M., K.M.S. is Funded by the Federal Ministry of Education and Research (BMBF) and the Ministry of Culture and Science of the German State of North Rhine-Westphalia (MKW) under the Excellence Strategy of the Federal Government and the Länder. K.M.S is supported by the NRW Rueckkehr Programme of the Ministry of Culture and Science of the German State of North Rhine-Westphalia (MKW). K.M.S. and F.K. were supported by grants from the Interdisciplinary Centre for Clinical Research (IZKF) within the faculty of Medicine at the RWTH Aachen University (OC1-9) and (PTD 1-11) respectively.

Conflicts of interest

None of the authors have a conflict of interest to declare that pertains to this work. Please refer to the accompanying ICMJE disclosure forms for further details.

Authors' contributions

Julius Werner Jaeger (Conceptualization: Supporting; Data curation: Lead; Formal analysis: Lead; Writing – original draft: Lead; Writing – review & editing: Equal). Annette Brandt (Data curation: Supporting; Formal analysis: Supporting; Methodology: Supporting; Writing – review & editing: Supporting). Wenfang Gui (Data curation: Supporting). Timur Yergalieyev (Formal analysis: Supporting; Investigation: Supporting; Methodology: Supporting). Angélica Hernández-Arriaga (Data curation: Supporting; Formal analysis: Supporting; Investigation: Supporting; Methodology: Supporting). Mukil Marutha Muthu (Data curation: Supporting; Formal analysis: Supporting; Investigation: Supporting; Methodology: Supporting). Ahmed Elashy (Data curation: Supporting). Karolina Edlund (Data curation: Supporting; Formal analysis: Supporting; Methodology: Supporting). Antonio Molinaro (Writing – review & editing: Supporting). Diana Möckel (Data curation: Supporting; Writing – review & editing: Supporting. Jan Philip Sarges (Data curation: Supporting). Jan Hengstler (Conceptualization: Supporting; Formal analysis: Supporting; Project administration: Supporting; Resources: Supporting; Supervision: Supporting; Writing – original draft: Supporting; Writing – review & editing: Supporting). Emelia Halibasic (Writing – review & editing: Supporting). Michael Trauner (Conceptualization: Supporting; Writing – review & editing: Supporting). Florian Kahles (Conceptualization: Supporting; Writing – review & editing: Supporting). Ulrike Rolle-Kampczyk (Data curation: Supporting; Formal analysis: Supporting; Investigation: Supporting; Methodology: Supporting). Carolin Victoria Schneider (Writing – review & editing: Supporting). Twan Lammers (Writing – review & editing: Supporting). Hanns-Ulrich Marschall (Conceptualization: Supporting; Funding acquisition: Lead; Project administration: Supporting; Resources: Supporting; Writing – review & editing: Supporting). Amelia Silva (Conceptualization: Supporting; Funding acquisition: Lead; Project administration: Supporting; Resources: Supporting; Writing – review & editing: Supporting). Martin von Bergen (Writing – review & editing: Supporting). Ina Bergheim (Conceptualization: Supporting; Funding acquisition: Lead; Project administration: Supporting; Resources: Supporting; Writing – review & editing: Supporting). Christian Trautwein MD (Conceptualization: Lead; Data curation: Equal; Formal analysis: Equal; Funding acquisition: Lead; Methodology: Lead; Project administration: Lead; Supervision: Lead; Validation: Equal; Writing – original draft: Supporting). Kai Markus Schneider, MD, PhD (Conceptualization: Lead; Data curation: Equal; Formal analysis: Equal; Funding acquisition: Lead; Methodology: Lead; Project administration: Lead; Supervision: Lead; Validation: Equal; Writing – original draft: Supporting).

Data availability statement

Data are available at reasonable request to the corresponding author. Single-cell RNA sequencing raw data is uploaded to ENA database (project ID PRJEB61876). RNA sequencing data is uploaded to GEO database (https://www.ncbi.nlm.nih.gov/geo/query/acc.cgi?acc=GSE246738).

Acknowledgments

We thank Ms. Sonja Strauch and Ms. Bettina Jansen—University Hospital RWTH Aachen, Aachen, Germany for their excellent technical assistance. We also acknowledge support by the High Performance and Cloud Computing Group at the Zentrum für Datenverarbeitung of the University of Tübingen, the state of Baden-Württemberg through bwHPC, and the German Research Foundation (DFG) through grant no. INST 37/935-1FUGG.

Supplementary data

Supplementary data to this article can be found online at https://doi.org/10.1016/j.jhepr.2023.100987.

References

Author names in bold designate shared co-first authorship

[1] **Loomba R**, **Friedman SL**, **Shulman GI**. Mechanisms and disease consequences of nonalcoholic fatty liver disease. Cell 2021;184:2537–2564.
[2] Attia SL, Softic S, Mouzaki M. Evolving role for pharmacotherapy in NAFLD/NASH. Clin Transl Sci 2021;14:11–19.
[3] **Wang R**, **Tang R**, Li B, et al. Gut microbiome, liver immunology, and liver diseases. Cell Mol Immunol 2020;18(1):4–17.
[4] **Schneider KM**, **Candels LS**, Hov JR, et al. Gut microbiota depletion exacerbates cholestatic liver injury via loss of FXR signalling. Nat Metab 2021;3(9):1228–1241.
[5] Schneider KM, Bieghs V, Heymann F, et al. CX3CR1 is a gatekeeper for intestinal barrier integrity in mice: limiting steatohepatitis by maintaining intestinal homeostasis. Hepatology 2015;62:1405–1416.
[6] Du B, Meenu M, Liu H, et al. A concise review on the molecular structure and function relationship of β-glucan. Int J Mol Sci 2019;20.
[7] Hughes SA, Shewry PR, Gibson GR, et al. In vitro fermentation of oat and barley derived β-glucans by human faecal microbiota. FEMS Microbiol Ecol 2008;64:482–493.
[8] Ellegård L, Andersson H. Oat bran rapidly increases bile acid excretion and bile acid synthesis: an ileostomy study. Eur J Clin Nutr 2007;61(8):938–945.
[9] Wang Y, Harding SV, Thandapilly SJ, et al. Barley β-glucan reduces blood cholesterol levels via interrupting bile acid metabolism. Br J Nutr 2017;118:822–829.
[10] Ho HVT, Sievenpiper JL, Zurbau A, et al. The effect of oat β-glucan on LDL-cholesterol, non-HDL-cholesterol and apoB for CVD risk reduction: a systematic review and meta-analysis of randomised-controlled trials. Br J

Nutr 2016;116:1369–1382. https://doi.org/10.1017/S000711451600341X. Preprint at.
[11] **Schneider KM**, **Elfers C**, Ghallab A, et al. Intestinal dysbiosis amplifies acetaminophen-induced acute liver injury. Cell Mol Gastroenterol Hepatol 2021;11:909.
[12] Gremse F, Stärk M, Ehling J, et al. Imalytics preclinical: interactive analysis of biomedical volume data. Theranostics 2016;6:328–341.
[13] **Schneider KM**, **Mohs A**, Gui W, et al. Imbalanced gut microbiota fuels hepatocellular carcinoma development by shaping the hepatic inflammatory microenvironment. Nat Commun 2022;13.
[14] Heymann F, Hammerich L, Storch D, et al. Hepatic macrophage migration and differentiation critical for liver fibrosis is mediated by the chemokine receptor C-C motif chemokine receptor 8 in mice. Hepatology 2012;55:898–909.
[15] Jung F, Staltner R, Baumann A, et al. A xanthohumol-rich hop extract diminishes endotoxin-induced activation of TLR4 signaling in human peripheral blood mononuclear cells: a study in healthy women. Int J Mol Sci 2022;23.
[16] Hernández-Arriaga A, Baumann A, Witte OW, et al. Changes in oral microbial ecology of C57BL/6 mice at different ages associated with sampling methodology. Microorganisms 2019;7:283.
[17] Bolyen E, Rideout JR, Dillon MR, et al. Reproducible, interactive, scalable and extensible microbiome data science using QIIME 2. Nat Biotechnol 2019;37(8):852–857.
[18] GitHub - najoshi/sabre. https://github.com/najoshi/sabre.
[19] Martin M. Cutadapt removes adapter sequences from high-throughput sequencing reads. EMBnet J 2011;17:10–12.
[20] Callahan BJ, McMurdie PJ, Rosen MJ, et al. DADA2: high-resolution sample inference from Illumina amplicon data. Nat Methods 2016;13(7):581–583.
[21] Robeson MS, O'Rourke DR, Kaehler BD, et al. RESCRIPt: reproducible sequence taxonomy reference database management for the masses. bioRxiv 2020. https://doi.org/10.1101/2020.10.05.326504.
[22] Rognes T, Flouri T, Nichols B, et al. VSEARCH: a versatile open source tool for metagenomics. PeerJ 2016 2016:e2584.
[23] Pedregosa Fabianpedregosa F, Michel V, Grisel Oliviergrisel O, et al. Scikit-learn: machine learning in Python Gaël Varoquaux Bertrand Thirion Vincent Dubourg Alexandre Passos PEDREGOSA, VAROQUAUX, GRAMFORT ET AL. Matthieu Perrot. J Machine Learn Res 2011;12:2825–2830.
[24] **Quast C**, **Pruesse E**, **Yilmaz P**, et al. The SILVA ribosomal RNA gene database project: improved data processing and web-based tools. Nucleic Acids Res 2013;41:D590–D596.
[25] Katoh K, Standley DM. MAFFT multiple sequence alignment software version 7: improvements in performance and usability. Mol Biol Evol 2013;30:772–780.
[26] Price MN, Dehal PS, Arkin AP. FastTree 2 – approximately maximum-likelihood trees for large alignments. PLoS One 2010;5:e9490.
[27] **Bray JR**, **Curtis JT**. An ordination of the upland forest communities of southern Wisconsin. Ecol Monogr 1957;27:325–349.
[28] Halko N, Martinsson PG, Shkolnisky Y, et al. An algorithm for the principal component analysis of large data sets. SIAM J Scientific Comput 2010;33:2580–2594.
[29] Anderson MJ. A new method for non-parametric multivariate analysis of variance. Austral Ecol 2001;26:32–46.
[30] Segata N, Izard J, Waldron L, et al. Metagenomic biomarker discovery and explanation. Genome Biol 2011;12:1–18.
[31] Patro R, Duggal G, Love MI, et al. Salmon provides fast and bias-aware quantification of transcript expression. Nat Methods 2017;14:417–419.
[32] Love MI, Soneson C, Hickey PF, et al. Tximeta: reference sequence checksums for provenance identification in RNA-seq. Plos Comput Biol 2020;16:e1007664.
[33] Love MI, Huber W, Anders S. Moderated estimation of fold change and dispersion for RNA-seq data with DESeq2. Genome Biol 2014;15:550.
[34] Wu T, Hu E, Xu S, et al. clusterProfiler 4.0: A universal enrichment tool for interpreting omics data. Innovation 2021;2:100141.
[35] Carlson M. org.Mm.eg.db: Genome wide annotation for Mouse. R package version 3.8.2. 2019. https://doi.org/10.18129/B9.bioc.org.Mm.eg.db. Preprint at.
[36] Yu G. enrichplot: Visualization of functional enrichment result. 2023. https://doi.org/10.18129/B9.bioc.enrichplot. Preprint at.
[37] Warnes G, Bolker B, Bonebakker L, et al. gplots: Various R programming tools for plotting data_. R package version 3.1.3. 2022. Preprint at, https://CRAN.R-project.org/package=gplots.
[38] Wickham H, Averick M, Bryan J, et al. Welcome to the Tidyverse. J Open Source Softw 2019;4:1686.
[39] Deng Q, She H, Cheng JH, et al. Steatohepatitis induced by intragastric overfeeding in mice. Hepatology 2005;42:905–914.
[40] Bruder-Nascimento T, Ekeledo OJ, Anderson R, et al. Long term high fat diet treatment: an appropriate approach to study the sex-specificity of the autonomic and cardiovascular responses to obesity in mice. Front Physiol 2017;8:32.
[41] Santhekadur PK, Kumar DP, Sanyal AJ. Preclinical models of nonalcoholic fatty liver disease. J Hepatol 2018;68:230.
[42] **Im YR**, **Hunter H**, de Gracia Hahn D, et al. A systematic review of animal models of NAFLD finds high-fat, high-fructose diets most closely resemble human NAFLD. Hepatology 2021;74:1884–1901.
[43] Winzell MS, Ahrén B. The high-fat diet-fed mouse: a model for studying mechanisms and treatment of impaired glucose tolerance and type 2 diabetes. Diabetes 2004;53(Suppl 3).
[44] **Bartneck M**, **Koppe C**, Fech V, et al. Roles of CCR2 and CCR5 for hepatic macrophage polarization in mice with liver parenchymal cell-specific NEMO deletion. Cell Mol Gastroenterol Hepatol 2021;11:327.
[45] Nogal A, Valdes AM, Menni C. The role of short-chain fatty acids in the interplay between gut microbiota and diet in cardio-metabolic health. Gut Microbes 2021;13.
[46] Ho HVT, Sievenpiper JL, Zurbau A, et al. The effect of oat β-glucan on LDL-cholesterol, non-HDL-cholesterol and apoB for CVD risk reduction: a systematic review and meta-analysis of randomised-controlled trials. Br J Nutr 2016;116:1369–1382.
[47] Suzuki S, Aoe S. High β-glucan barley supplementation improves glucose tolerance by increasing glp-1 secretion in diet-induced obesity mice. Nutrients 2021;13:1–11.
[48] Choi JS, Kim H, Jung MH, et al. Consumption of barley β-glucan ameliorates fatty liver and insulin resistance in mice fed a high-fat diet. Mol Nutr Food Res 2010;54:1004–1013.
[49] Kei N, Wong VWS, Lauw S, et al. Utilization of food-derived β-glucans to prevent and treat non-alcoholic fatty liver disease (NAFLD). Foods 2023;12:3279.
[50] Ho HVT, Sievenpiper JL, Zurbau A, et al. The effect of oat β -glucan on LDL-cholesterol, non-HDL-cholesterol and apoB for CVD risk reduction: a systematic review and meta-analysis of randomised-controlled trials. Br J Nutr 2016;116:1369–1382.
[51] Mio K, Yamanaka C, Matsuoka T, et al. Effects of β-glucan rich barley Flour on glucose and lipid metabolism in the ileum, liver, and adipose tissues of high-fat diet induced-obesity model male mice analyzed by DNA microarray. Nutrients 2020;12(3546):3546.
[52] Vitaglione P, Lumaga RB, Stanzione A, et al. Beta-Glucan-enriched bread reduces energy intake and modifies plasma ghrelin and peptide YY concentrations in the short term. Appetite 2009;53:338–344.
[53] Wolever TMS, Tosh SM, Spruill SE, et al. Increasing oat β-glucan viscosity in a breakfast meal slows gastric emptying and reduces glycemic and insulinemic responses but has no effect on appetite, food intake, or plasma ghrelin and PYY responses in healthy humans: a randomized, placebo-controlled, crossover trial. Am J Clin Nutr 2020;111:319–328.
[54] **Qin N**, **Yang F**, **Li A**, et al. Alterations of the human gut microbiome in liver cirrhosis. Nature 2014;513(7516):59–64.
[55] **Bashiardes S**, **Shapiro H**, **Rozin S**, et al. Non-alcoholic fatty liver and the gut microbiota. Mol Metab 2016;5:782–794.
[56] Boursier J, Mueller O, Barret M, et al. The severity of nonalcoholic fatty liver disease is associated with gut dysbiosis and shift in the metabolic function of the gut microbiota. Hepatology 2016;63:764–775.
[57] **Lee G**, **You HJ**, Bajaj JS, et al. Distinct signatures of gut microbiome and metabolites associated with significant fibrosis in non-obese NAFLD. Nat Commun 2020;11:1–13.
[58] Cheng WY, Lam KL, Li X, et al. Circadian disruption-induced metabolic syndrome in mice is ameliorated by oat β-glucan mediated by gut microbiota. Carbohydr Polym 2021;267.
[59] Tsai M-C, Liu Y-Y, Lin C-C, et al. Gut microbiota dysbiosis in patients with biopsy-proven nonalcoholic fatty liver disease: a cross-sectional study in taiwan. Nutrients 2020;12:820.

[60] Hrncir T, Hrncirova L, Kverka M, et al. Gut microbiota and NAFLD: pathogenetic mechanisms, microbiota signatures, and therapeutic interventions. Microorganisms 2021;9:957.
[61] Seki E, De Minicis S, Österreicher CH, et al. TLR4 enhances TGF-β signaling and hepatic fibrosis. Nat Med 2007;13:1324–1332.
[62] Schneider KM, Bieghs V, Heymann F, et al. CX3CR1 is a gatekeeper for intestinal barrier integrity in mice: limiting steatohepatitis by maintaining intestinal homeostasis. Hepatology 2015;62:1405–1416.
[63] Miura K, Kodama Y, Inokuchi S, et al. Toll-like receptor 9 promotes steatohepatitis by induction of interleukin-1β in mice. Gastroenterology 2010;139:323–334.e7.
[64] Scientific Opinion on the substantiation of a health claim related to oat beta glucan and lowering blood cholesterol and reduced risk of (coronary) heart disease pursuant to Article 14 of Regulation (EC) No 1924/2006. EFSA J 2010;8.
[65] Chang HC, Huang CN, Yeh DM, et al. Oat prevents obesity and abdominal fat distribution, and improves liver function in humans. Plant Foods Hum Nutr 2013;68:18–23.
[66] **Wang N**, **Liu H**, Liu G, et al. Yeast β-D-glucan exerts antitumour activity in liver cancer through impairing autophagy and lysosomal function, promoting reactive oxygen species production and apoptosis. Redox Biol 2020;32:101495.